Theor Chem Acc (2000) 104:131–139
DOI 10.1007/s002140000115

Theoretical
Chemistry Accounts

Regular article

The Ti_2H_2 molecule: terminal or bridging hydrogens ?

Imre Pápai

Institute of Isotope and Surface Chemistry, Spectroscopy Department, Chemical Research Centre, HAS, P.O. Box 77, 1525 Budapest, Hungary

Received: 15 September 1999 / Accepted: 7 December 1999 / Published online: 19 April 2000

Abstract. Density functional calculations carried out for Ti_2H_2 show that several structures are thermodynamically stable with respect to $Ti_2 + H_2$. The ground state of Ti_2H_2 is found to be $^3B_1$ and it involves two hydrogen bridges in a nonplanar C_{2v} arrangement. The $^1A_1$ state and other triplet states of the bridging structure are only a few kilocalories per mole above the ground state. The $^1\Sigma_g^+$ state, which corresponds to the Ti analogue of acetylene, is energetically less favored than the bridging structure but it is still bound relative to $Ti_2 + H_2$. Results are also presented for the Ti_2H molecule. Both bridging and terminal isomers are found to be very stable due to the formation of strong covalent Ti—H bonds. A comparison of the calculated harmonic vibrational frequencies and IR intensities of Ti_2H_2 and Ti_2H isomers with the spectra from matrix isolation IR studies on Ti_x/H_2 indicates that these molecules may have been produced in low-temperature reactions.

Key words: Density functional theory – Ti_2H_2 – Ti_2H – Transition-metal hydrides

1 Introduction

We have recently identified two new titanium hydride species – $HTi(C_2H_3)$ and $H_2Ti(C_2H_2)$ – which were formed in the reactions of Ti atoms with ethylene in Ar matrices [1]. The singlet states of these species were characterized as titana-cyclopropenes since their structures were analogous to C_3H_4. The $H_2Ti(C_2H_2)$ molecule can formally be derived from C_3H_4 by replacing the sp^3 carbon atom by a four-valent Ti atom, while in $HTi(C_2H_3)$, one of the sp^2 carbons is substituted by Ti (see Fig. 1).

There are a few other examples that indicate a close structural resemblance between simple hydrocarbons and their titana analogues. The titane molecule (TiH_4), for example, is known to exist in the gas phase at room temperature [2] and its equilibrium structure is predicted to be tetrahedral [3, 4]. The ground state of TiH_2 is found to be triplet with a bent equilibrium geometry [5, 6], showing similarity with the CH_2 radical. The reason for these structural analogies lies in the fact that both Ti and C have four valence electrons and their ground states are associated with similar electron configurations (s^2d^2 and s^2p^2).

The TiH_4 molecule has also been produced in low-temperature rare-gas matrices and it has been characterized by IR spectroscopy [7, 8]. First, Xiao et al. [7] observed that the photolysis of matrix deposits obtained by trapping thermally vaporized Ti and H_2 gave TiH_4, as well as TiH_2. Chertihin and Andrews [8] later used laser-ablated Ti to react with hydrogen in argon and tried to identify all four members in the TiH_x ($x = 1–4$) series among the reaction products. Both matrix isolation experiments, however, indicated that in addition to TiH_x species, titanium hydrides with higher Ti stochiometry were also produced in the reactions. No attempts were made to identify these Ti_xH_y species, but the existence of broad features in the IR spectra around 1500 cm^{-1} [7, 8], 1400 cm^{-1} [7] and 1250 cm^{-1} [8] suggested that two types of bound hydrogens (terminal and bridging) exist in the Ti_xH_y molecules [8] and that the geometry of these clusters may not be well defined [7]. These conclusions were indeed supported by recent quantum chemical studies on Ti_2H_8 and Ti_2H_6 clusters [9–11]. The results obtained at various post-Hartree–Fock levels for these systems revealed a number of close-lying stable isomers which always involved both terminal and bridging hydrogens. Webb and Gordon [9, 11] considered these Ti_2H_{2n} species as possible reaction products in the matrix isolation experiments and assumed that they were formed by the dimerization of TiH_3 and TiH_4.

The present theoretical work is devoted to the simplest Ti_2H_{2n} species, the Ti_2H_2 molecule, which may be derived from the reaction of Ti_2 with molecular hydrogen. It is shown that Ti_2H_2 may exist in several structural forms, of which one is identified as the titana analogue of the acetylene molecule.

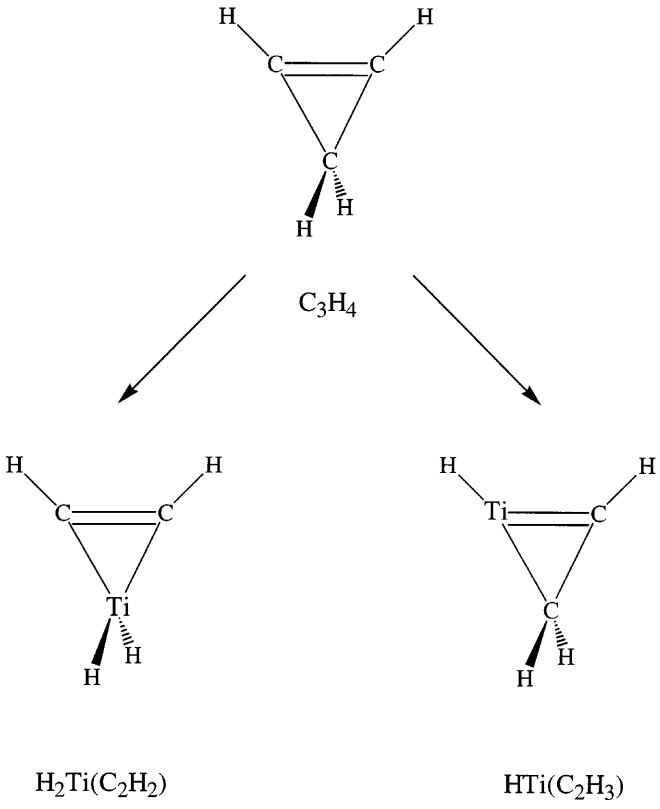

Fig. 1. Structure of the $H_2Ti(C_2H_2)$ and $HTi(C_2H_3)$ molecules

2 Computational method

The calculations in this work were carried out within the density functional formalism using the Gaussian94 package [12]. The (14,9,5)/[8,5,3] all-electron basis set of Thomass et al. [13] supplemented with two polarization p functions [14] and a diffuse d function [15] was chosen to describe the Ti atom, while a standard TZ2P basis from the 6-311G(2d,2p) set [12] was used for H.

Three frequently used exchange–correlation functionals were chosen to solve the Kohn–Sham equations. Namely, the B3LYP, BLYP and BP86 functionals, where B3LYP is Becke's three parameter hybrid exchange functional [16] combined with the correlation functional of Lee, Yang and Parr (LYP) [17], while in BLYP and BP86, B refers to Becke's 1988 exchange functional [18] and P86 is Perdew's 1986 gradient-corrected correlation functional [19].

The geometries of the systems studied were always fully optimized using the Berny algorithm [20]. The harmonic vibrational frequencies were obtained from analytic energy second derivatives. The stabilities of various forms of Ti_2H_2 are given with respect to $Ti_2 + H_2$. The dissociation energies were always corrected for the zero-point-energy contributions determined from BP86 harmonic frequencies.

3 Results and discussion

3.1 The H_2, Ti_2, TiH and TiH_4 molecules

First of all, results for the ground states of Ti_2 and H_2 are presented. The equilibrium bond lengths and the harmonic vibrational frequencies obtained with the three functionals are listed in Table 1. It is also important to see how these functionals perform for systems involving Ti—H bonds; therefore, in Table 1 results for TiH and TiH_4 are also included.

While the equilibrium properties of H_2 [21] are well reproduced with all functionals, this is not quite true for the Ti_2 dimer, which has always been a challenge for quantum chemical calculations [22–24]. The ground state of Ti_2 is $^3\Delta_g$ [25] and its equilibrium bond length, R_e, and its equilibrium harmonic vibrational frequency, ω_e, are known from resonant two-photon ionization [25] and resonance Raman [26] spectroscopic studies. The $^3\Delta_g$ state is predicted to be the ground state at the present levels of density functional theory (DFT). The lowest singlet and quintet states are calculated to be about 9–13 kcal/mol above $^3\Delta_g$, while the $^7\sum_u$ state is predicted to lie even higher in energy (14–19 kcal/mol above the ground state). Table 1 shows that the B3LYP functional underestimates the equilibrium bond length of the $^3\Delta_g$ state by 0.03 Å and overestimates its ω_e by about 20%. The bond lengths and harmonic frequencies obtained with the generalized gradient approximation (GGA) functionals (BLYP and BP86) are all closer to the experimental values of 1.942 Å and 408 cm^{-1}.

All three functionals predict the $^4\Phi$ state to be the ground state of TiH. The results are fairly stable with respect to the functional applied and they show a slight variation from those of a recent DFT study [27] carried out with a somewhat smaller basis set. The calculated bond lengths are about 0.03 Å shorter than the experimental value (1.785 Å [28]). The discrepancy between theory and experiment seems to be more severe for ω_e, since all DFT predictions are much higher than the experimental IR absorption at 1385 cm^{-1}, which was assigned to TiH by Chertihin and Andrews [8]. It is quite clear that the present DFT methodology, which does not account for near-degeneracy electron correlation, might not be sufficient to give very accurate predictions for the open shell $6\sigma^2 7\sigma^1 3\pi^1 1\delta^1$ configuration associated with the $^4\Phi$ state of TiH, but the underestimation of R_e by 0.03 Å certainly does not cause an error of 200 cm^{-1} in the harmonic frequency. Moreover, most of the extensive correlated ab initio calculations [29–31] also predict $\omega_e > 1500\,cm^{-1}$. For instance, Bauschlicher's full configuration interaction benchmark calculations [30] gave $\omega_e = 1572\,cm^{-1}$, again far from experiment. These results indicate that the observed 1385 cm^{-1} band might not be due to TiH.

No experimental data are available for the TiH bond length in TiH_4, but the results obtained with the three functionals are all close to 1.71 Å, which is equal to the value predicted by the coupled-cluster single-double excitation method [4]. The TiH stretching frequencies are more sensitive to the functional since the B3LYP values for both symmetric and asymmetric TiH stretching vibrations are $60-70\,cm^{-1}$ higher than those of BLYP and BP86. The latter mode is IR active and it has been observed at 1666 cm^{-1} [7] and 1664 cm^{-1} [8] in Ar matrices. The BLYP and BP86 predictions for this mode appear to be fairly accurate, whereas B3LYP slightly overestimates the observed value. This trend would be the same if corrections for anharmonicity and matrix effects were considered.[1]

[1] This correction altogether is expected to be around $20-30\,cm^{-1}$

Table 1. Ground-state properties of H_2, Ti_2, TiH and TiH_4: bond lengths, R_e, (Å), the harmonic vibrational frequencies ω_e, (cm^{-1}) and the IR intensities in *parentheses*, (km/mol)

	B3LYP	BLYP	BP86	Exp.
H_2 ($^1\Sigma_g^+$)				
R_e	0.743	0.746	0.751	0.742[a]
ω_e	4422	4353	4319	4395[a]
Ti_2 ($^3\Delta_g$)				
R_e	1.912	1.958	1.934	1.942[b]
ω_e	484	426	434	408[c]
TiH ($^4\Phi$)				
R_e	1.760	1.760	1.752	1.785[d]
ω_e	1575	1556	1572	1385[e]
TiH_4 ($^1A_1$)				
R_e	1.698	1.714	1.711	–
$\omega_1(a_1)$	1790 (0)	1715 (0)	1717 (0)	–
$\omega_2(t_2)$	1730 (426)	1672 (327)	1676 (327)	1666[f]
$\omega_3(e)$	622 (0)	614 (0)	582 (0)	–
$\omega_4(t_2)$	538 (150)	543 (146)	525 (159)	–

[a] Ref. [21]
[b] Ref. [25]
[c] Ref. [26]
[d] Ref. [27]
[e] Ref. [8]
[f] Ref. [7]

In summary, all three functionals perform reasonably well for the systems presented, except that B3LYP gives slight overestimations for both TiTi and TiH stretching frequencies. For further calculations, all three functionals were used to determine the equlibrium geometries and the relative energies, but for the vibrational analysis of the structures obtained only BP86 calculations were carried out.

3.2 The Ti_2H_2 molecule: various forms

Given that hydrogen atoms may form terminal and bridging Ti—H bonds with Ti_2, four types of structural isomers are considered for Ti_2H_2. These structures are depicted in Fig. 2. The HTiTiH and H_2TiTi isomers have only terminal hydrogens and they are the titana analogues of the acetylene molecule and the vinylidene radical. The latter structure, however, could not be located either on the triplet or on the singlet Ti_2H_2 potential-energy surfaces. Starting from a number of initial structures corresponding to H_2TiTi, the geometry-optimization procedure always led to the formation of bridging hydrogens. The Ti(H,H)Ti isomer has two bridging hydrogens, while the Ti(H)TiH structure involves one bridging and one terminal hydrogen. The equilibrium geometries and the dissociation energies of the located structures are given in Tables 2–4.

The ground state ($^1\Sigma_g^+$) of the HTiTiH molecule is linear and it is thermodynamically stable with respect to the $Ti_2(^3\Delta_g) + H_2(^1\Sigma_g^+)$ dissociation limit (Table 2). The BLYP and BP86 dissociation energies range between 7 and 9 kcal/mol, while B3LYP predicts $\Delta E = 13.6$ kcal/mol. The TiTi bond length in HTiTiH hardly differs from that in the ground state of Ti_2, and the predicted TiH distances are between those in TiH and TiH_4. The triplet states of HTiTiH are calculated to be unstable since the dissociation energies are close to zero.

The singlet–triplet splitting is much smaller for the Ti(H,H)Ti form of Ti_2H_2 (Table 3). All functionals predict the triplet $^3B_1$ state to be the ground state, but the lowest singlet state ($^1A_1$) lies only a few kilocalories per mole above $^3B_1$. The dissociation energies for these states are 21–25 kcal/mol (for $^1A_1$) and 23–30 kcal/mol (for $^3B_1$), showing that the Ti(H,H)Ti structure is notably more stable than HTiTiH. In both the $^3B_1$ and the $^1A_1$ states, the TiH bond lengths are around 1.87 Å, which is about 0.13 Å longer than the terminal bonds. The TiTi distance in Ti(H,H)Ti is significantly larger than in HTiTiH and it shows a variance for the $^3B_1$ and $^1A_1$ states: the distances are about 0.04–0.05 Å shorter in the

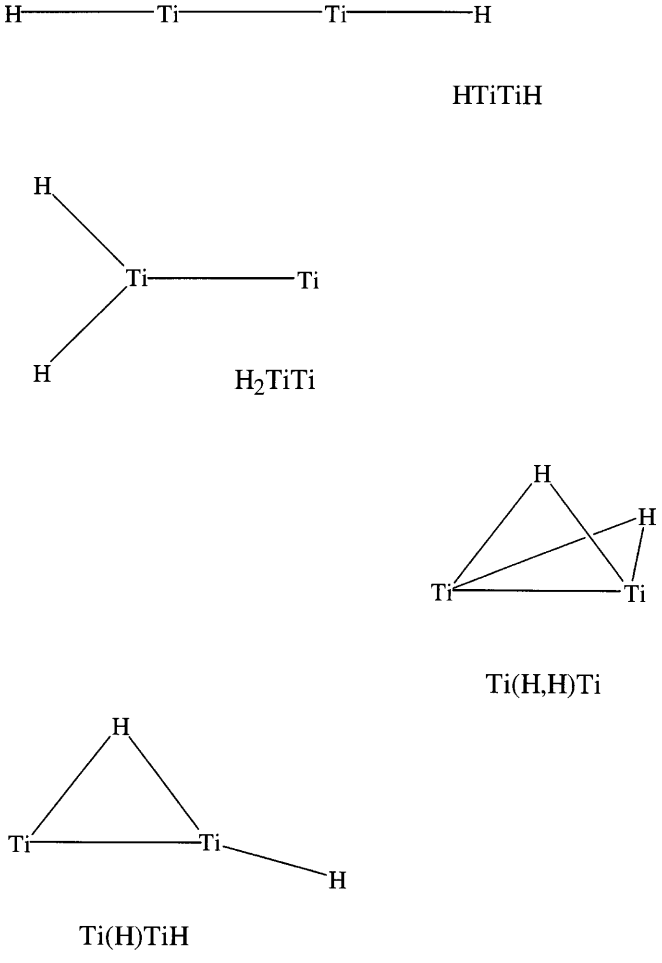

Fig. 2. Possible Ti_2H_2 isomers

Table 2. Equilibrium structural parameters and dissociation energies for the HTiTiH structure of Ti_2H_2: bond lengths, R, (Å) and the dissociation energies, ΔE, (kcal/mol) with respect to $Ti_2(^3\Delta_g) + H_2(^1\Sigma_g^+)$

$^1\Sigma_g^+$ state ($D_{\infty h}$)	B3LYP	BLYP	BP86
R(TiTi)	1.915	1.951	1.936
R(TiH)	1.732	1.744	1.736
ΔE	13.6	7.3	8.4

Table 3. Equilibrium structural parameters and dissociation energies for the Ti(H,H)Ti structure of Ti_2H_2: R (Å), angles, α(HXH), in degrees and ΔE (kcal/mol) with respect to $Ti_2(^3\Delta_g) + H_2(^1\Sigma_g^+)$. X in α(HXH) denotes the midpoint of the Ti—Ti bond

	B3LYP	BLYP	BP86
$^1A_1$ state (C_{2v})			
R(TiTi)	2.010	2.044	2.029
R(TiH)	1.871	1.876	1.866
α(HXH)	91.4	91.6	91.3
ΔE	20.9	21.8	25.4
$^3B_1$ state (C_{2v})			
R(TiTi)	2.049	2.089	2.074
R(TiH)	1.873	1.877	1.865
α(HXH)	124.1	124.6	125.5
ΔE	23.2	25.2	29.5

Table 4. Equilibrium structural parameters and dissociation energies for the HTi(H)Ti structure of Ti_2H_2: R (Å), α(HXH) in degrees and ΔE (kcal/mol) with respect to $Ti_2(^3\Delta_g) + H_2(^1\Sigma_g^+)$. R_1 refers to terminal, R_2 and R_2' to bridging Ti—H bonds (R_2' is associated with Ti that binds the terminal hydrogen (H^t))

	B3LYP[a]	BLYP	BP86
$^1A'$ state (C_s)			
R(TiTi)	1.942	1.921	1.896
R_1(TiH)	1.745	1.743	1.736
R_2(TiH)	1.796	1.853	1.839
R_2'(TiH)	1.834	1.896	1.898
α(TiTiH^t)	178.3	181.1	178.8
ΔE	−8.4[b]	8.2	10.4
$^3A'$ state (C_s)			
R(TiTi)	–	2.088	2.056
R_1(TiH)	–	1.802	1.795
R_2(TiH)	–	1.847	1.840
R_2'(TiH)	–	1.905	1.889
α(TiTiH^t)	–	157.1	161.8
ΔE	–	13.8	16.3

[a] Geometry optimization carried out with the B3LYP functional for the $^3A'$ state converges to the Ti(H,H)Ti form

[b] The negative sign indicates that HTi(H)Ti is predicted to be unstable

singlet state. Surprisingly, the Ti(H,H)Ti molecule is not planar. The D_{2h} arrangement of the bridging hydrogens is a transition state on the potential-energy hypersurface. The two TiHTi planes in the equilibrium structure of the $^1A_1$ state meet at about a right angle, α(HXH)$\approx 90°$, while this angle is about 125° for the ground state. This structure is very similar to that found for the dibridged disilyne, Si(H_2)Si, molecule [32]. It should be mentioned here that a few other triplet states are predicted to lie close to the $^3B_1$ state. For instance, BP86 calculations predict the $^3A_1$ state to be 4 kcal/mol above the $^3B_1$ state with R(TiTi) = 1.953 Å, R(TiH) = 1.884 Å and α(HXH) = 108.4° equilibrium parameters.

Table 5. Dissociation energies (kcal/mol) of various forms of Ti_2H_2

	B3LYP	BLYP	BP86
HTiTiH			
$^1\Sigma_g^+$	13.6	7.3	8.4
Ti(H,H)Ti			
$^1A_1$	20.9	21.8	25.4
$^3B_1$	23.2	25.2	29.5
HTi(H)Ti			
$^1A'$	−8.4	8.2	10.4
$^3A'$	–	13.8	16.3

For the Ti(H)TiH isomer, the B3LYP and the GGA results are quite different (Table 4). While the BLYP and BP86 dissociation energies for the $^1A'$ and $^3A'$ states are calculated to be between those of HTiTiH and Ti(H,H)Ti, the B3LYP functional predicts this form to be unstable with respect to $Ti_2 + H_2$. From the B3LYP results, the $^1A'$ state is 8 kcal/mol above the dissociation limit, and for the $^3A'$ state, B3LYP does not even yield an energy minimum since the geometry optimization converges to the Ti(H,H)Ti structure. The normal coordinate analysis of the vibrational modes carried out at the BLYP and BP86 levels for the located $^3A'$ minima shows that both in-plane and out-of-plane TiTiH^t bending frequencies are rather low (about 200 cm^{-1}). It appears then that the discrepancy between the B3LYP and GGA results for the $^3A'$ state originates in the flat character of the potential-energy surface in the region. All located Ti(H)TiH structures are planar with nearly linear TiTiH^t parts for the singlet and with α(TiTiH^t) $\approx$ 160° for the $^3A'$ state.

The dissociation energies of the located forms of Ti_2H_2 are collected in Table 5. They clearly show that the Ti(H,H)Ti structure is energetically favored over the HTiTiH and Ti(H)TiH isomers, with a slight preference for the triplet state. The other two structures are notably less stable, but they are generally bound with respect to $Ti_2 + H_2$. Although the $^3A'$ state of Ti(H)TiH is found to be lower in energy than the $^1A'$ state, the existence of the triplet Ti(H)TiH structure is uncertain. Even if it is a minimum on the triplet surface, it may convert easily to the dibridging form.

Before we proceed to analyze the nature of the bonding in the located Ti_2H_2 isomers, the interaction of a single H atom with the ground state of Ti_2 will be discussed.

3.3 The Ti_2H molecule: structure and bonding

A single H atom is able to bind in both end-on and side-on ways to Ti_2, resulting in linear TiTiH and bridging

Ti(H)Ti molecules. The ground states of these forms are predicted to be $^2\Delta$ and $^4B_1$, respectively. While the quartet states of TiTiH are well separated from the ground state, the doublet states of Ti(H)Ti, of which $^2B_1$ is the lowest, lie very close to $^4B_1$. The calculated properties for the $^2\Delta$, $^4B_1$ and $^2B_1$ states of Ti_2H are presented in Table 6.

All functionals predict the $^4B_1$ state to be the most stable state followed by the $^2B_1$ and $^2\Delta$ states. The binding energy of the H atom in $^4B_1$ is between 60 and 66 kcal/mol, but it is also close to 60 kcal/mol in the TiTiH ($^2\Delta$) molecule, showing that both terminal and bridging hydrogens are strongly bound to Ti_2. For the terminal Ti—H bond, R(TiH) = 1.74 Å, while the bridging bonds are roughly 0.1 Å longer. The metal–metal bond becomes shorter in TiTiH and lengthens in Ti(H)Ti compared to that in Ti_2 ($^3\Delta_g$). Consequently, the TiTi stretching vibrational frequency shifts to a higher value in TiTiH and the frequencies are lower in the $^4B_1$ and $^2B_1$ states of Ti(H)Ti than in Ti_2. The terminal TiH stretching frequency is predicted to be between 1520 and 1560 cm^{-1}, while the symmetric TiH stretching modes in the Ti(H)Ti states are around 1400 cm^{-1}. The calculated asymmetric TiH stretching frequencies are around 1000 cm^{-1} in $^4B_1$ and a bit higher (about 1100 cm^{-1}) in $^2B_1$ states.

To describe the bonding in TiTiH and Ti(H)Ti, let us first recall that the $^3\Delta_g$ state of Ti_2 is associated with the $1\sigma_g^2\pi_u^4 2\sigma_g^1\delta^1$ configuration of valence electrons [23]. Here, the fully occupied $1\sigma_g$ and π_u orbitals represent 4*s*-4*s* and $3d_\pi$-$3d_\pi$ bonding overlaps, whereas the singly occupied $2\sigma_g$ and δ are $3d_\sigma$-$3d_\sigma$ and $3d_\delta$-$3d_\delta$ bonding overlaps (Fig. 3). All these two- and one-electron combinations give rise to a quadruple metal–metal bond in $Ti_2(^3\Delta_g)$.

Table 6. Structural parameters, dissociation energies and IR spectra of various states of Ti_2H: R (Å), ΔE (kcal/mol) with respect to $Ti_2(^3\Delta_g) + H(^2S)$, harmonic frequencies, ω_i (cm^{-1}) and IR intensities in *parentheses*) (km/mol)

	B3LYP	BLYP	BP86
TiTiH ($^2\Delta$)			
R(TiTi)	1.862	1.895	1.875
R(TiH)	1.736	1.745	1.738
ΔE	56.4	54.3	56.2
$\omega_1(\sigma)$	1563 (594)	1527 (445)	1536 (445)
$\omega_2(\sigma)$	574 (89)	531 (71)	559 (76)
$\omega_3(\pi)$	478 (72)	473 (53)	482 (54)
Ti(H)Ti ($^2B_1$)			
R(TiTi)	2.039	2.058	2.042
R(TiH)	1.831	1.846	1.832
ΔE	59.3	58.2	63.0
$\omega_1(a_1)$	1434 (49)	1368 (53)	1409 (46)
$\omega_2(b_2)$	1159 (41)	1086 (23)	1146 (47)
$\omega_3(a_1)$	464 (3)	390 (3)	388 (3)
Ti(H)Ti ($^4B_1$)			
R(TiTi)	1.971	2.029	1.991
R(TiH)	1.850	1.854	1.845
ΔE	60.2	61.6	65.8
$\omega_1(a_1)$	1417 (60)	1373 (56)	1397 (56)
$\omega_2(b_2)$	1083 (152)	1010 (27)	1039 (32)
$\omega_3(a_1)$	397 (6)	343 (2)	355 (3)

The $^2\Delta$, $^4B_1$ and $^2B_1$ states of Ti_2H can be derived from the ground states of Ti_2 and H since all three states dissociate into $Ti_2(^3\Delta_g) + H(^2S)$. The dissociation energy curves, derived at the BP86 level by varying the Ti—H distances with fixed R(TiTi) values, are depicted in Fig. 4. The analysis of the Kohn–Sham orbitals of various TiTiH and Ti(H)Ti structures along the dissociation curves reveals the bonding mechanisms in the two forms. The singlet pairing of the hydrogen 1*s* and Ti_2 $2\sigma_g$ electrons gives rise to a covalent Ti—H bond in TiTiH ($^2\Delta$). The doubly occupied σ Ti—H bonding orbital (Fig. 5) has about 60% 1*s*(H) character, indicating a slight charge transfer from Ti_2 to H. This orbital is the lowest lying TiTiH valence orbital and is well separated from the pure Ti_2 ($1\sigma_g, \pi_u$ and δ) orbitals. The mixing of 1*s*(H) with the unpaired $Ti_2 2\sigma_g$ and δ orbitals is unfavored in the Ti(H)Ti isomer, but 1*s*(H) can interact with the more diffuse and doubly occupied $1\sigma_g$ orbital. To decrease the two-orbital three-electron repulsive interaction between the occupied orbitals (Pauli repulsion), the metal 4*s* electrons polarize away from H through mixing of $1\sigma_g$ with the in-plane component of π_u and, on the other hand, 4*s* electrons are excited to an empty metal orbital. The excitation can take place either in the majority or in the minority spin orbital space leading to the $^4B_1$ and $^2B_1$ states, respectively. In their equilibrium structures, the Ti—H bonding orbitals of $^4B_1$ and $^2B_1$ are the lowest-lying valence orbitals, which are doubly occupied three-center a_1 orbitals, again having 60% 1*s*(H) and 40% Ti_2 ($1\sigma_g + \pi_u$) character (Fig. 5).

We see that the terminal and the bridging Ti—H bonds in the two forms of Ti_2H are strong covalent bonds with slight ionic character. The formation of these bonds, however, has a different influence on the strength of the Ti—Ti bond. Since the Ti 4*s* and $3d_\pi$ electrons become involved in the Ti—H bonds in Ti(H)Ti, the metal–metal interaction is weakened with respect to that in $Ti_2(^3\Delta_g)$. Although the σ(Ti—H) bonding orbital in TiTiH has a nonnegligible Ti 4*s* admixture, the $3d_\pi$-$3d_\pi$ bond is unaffected in this form.

3.4 Bonding in HTiTiH and Ti(H,H)Ti

The TiTiH ($^2\Delta$) molecule can bind a second H atom on the other side of the Ti_2 without loosening the 4*s*-4*s* and $3d_\pi$-$3d_\pi$ metal–metal bonds. Although the $3d_\sigma$-$3d_\sigma$ is weakened because the σ_u combination of the two Ti-H overlaps is Ti—Ti antibonding (Fig. 6), the Ti_2 $1\sigma_g(4s)$ and $\pi_u(3d_\pi)$ orbitals are practically unchanged when going from $Ti_2(^3\Delta_g)$ to $HTiTiH(^1\Sigma_g^+)$. This type of bonding is analogous to that in acetylene in that both molecules have strong covalent X—H bonds and the heavy atoms are linked through a triple bond. The main difference between the highest occupied molecular orbital and the lowest unoccupied molecular orbital is that the π components of the Ti ≡ Ti bond are due to *d*-type orbitals, while they are a result of *p*-*p* overlaps in C_2H_2. For this reason, the energy difference between the highest occupied molecular orbital and the lowest unoccupied molecular orbital is much smaller in HTiTiH (around 0.7 eV versus around 7 eV in C_2H_2), but it is

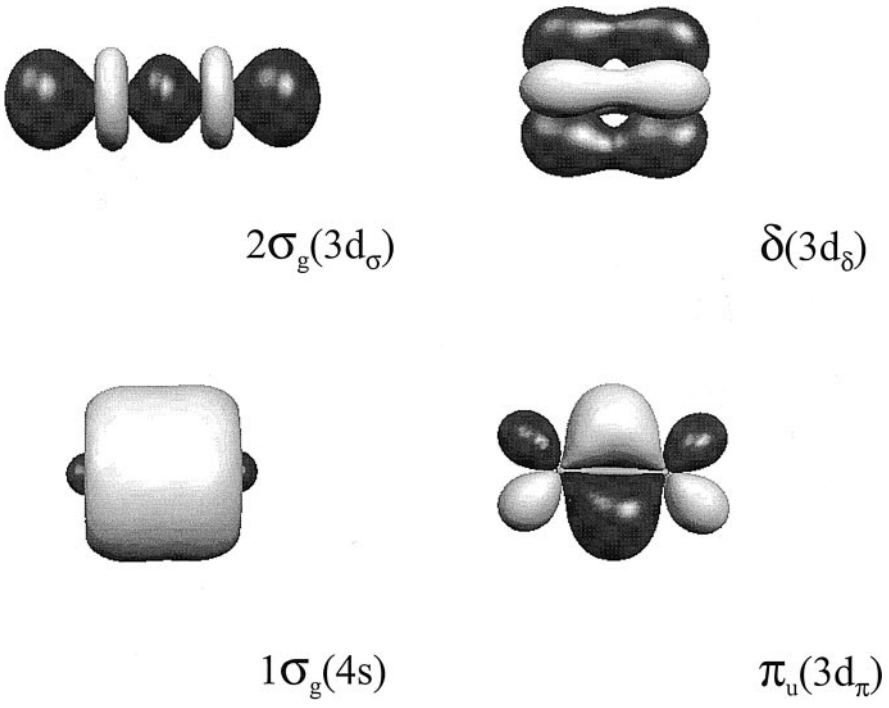

Fig. 3. Valence orbitals of $Ti_2(^3\Delta_g)$. (Plotted with the Molekel visualization program [33])

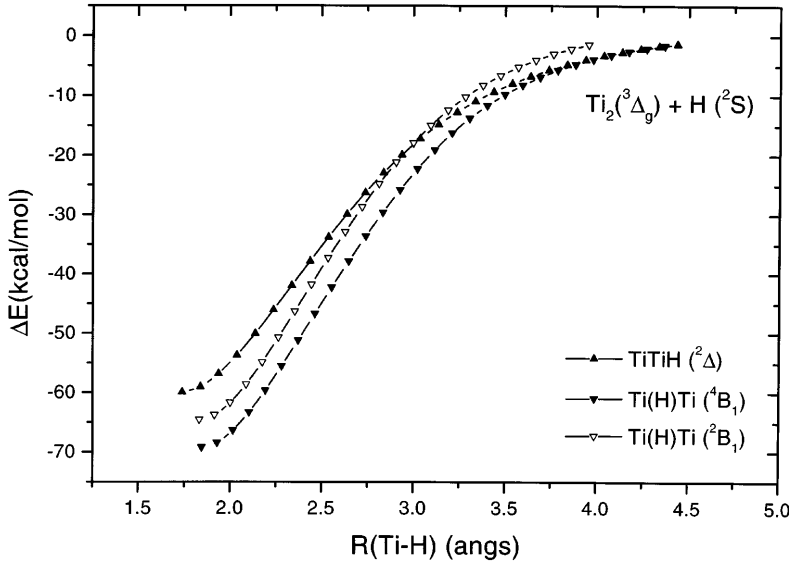

Fig. 4. Dissociation of TiTiH($^2\Delta$) and Ti(H)Ti ($^4B_1$ and $^2B_1$). R(TiTi) are 1.875, 1.991 and 2.042 Å for the $^2\Delta$, $^4B_1$ and $^2B_1$ states, respectively. Energies are calculated relative to $Ti_2(^3\Delta_g)$ + H(^{2}S)

still sufficient to separate the singlet ground state from the triplets. The existence of the triple bond between the Ti atoms is unambiguously confirmed by calculating the Mayer bond orders [34–36]. For the Ti—Ti overlap, the Mayer bond order is very close to 3.0 and is independent of the functional applied.

The Ti—Ti bond is much weaker in the Ti(H,H)Ti molecule, since due to the nonplanar arrangement of the H atoms both $\pi_u(3d_\pi)$ components of Ti_2 contribute to the Ti—H bonds (Fig. 7). In the planar Ti(H,H)Ti structure, the symmetric (+ +) combination of 1s(H) orbitals does not overlap with the in-plane $\pi_u(3d_\pi)$ Ti_2 orbital for symmetry reasons, so this structure is energetically less favored. The $1s(\mathrm{H})-\pi_u(3d_\pi)$ (Ti_2) overlap is maximized at $\alpha(\mathrm{HXH}) = 90°$, which is apparent in the equilibrium structure of the $^1A_1$ state. In the ground state ($^3B_1$) of Ti(H,H)Ti, the presence of a singly occupied a_1 orbital, which is a Ti_2 $\delta(3d_\delta)$ orbital (Fig. 3), pushes apart the hydrogen atoms due to Pauli repulsion. Consequently, the α(HXH) angle in the $^3B_1$ state is an obtuse angle (around 125°).

The Ti—Ti bond would undergo further weakening if additional H atoms were attached to Ti_2H_2. Preliminary results for Ti_2H_4 indicate considerable metal–metal overlaps in both double and quadruple hydrogen-bridged structures [HTi(H,H)TiH and Ti(H,H,H,H)Ti in our notation], but as shown by Webb and Gordon [9, 11], there is only little or no direct bonding between the

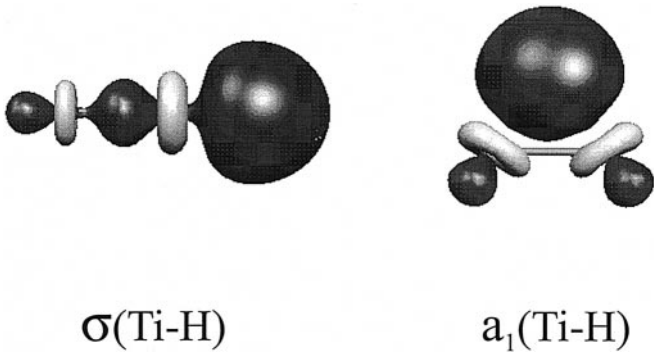

Fig. 5. Ti—H bonding orbitals of TiTiH [σ(Ti—H)] and Ti(H)Ti [a_1(Ti—H)]

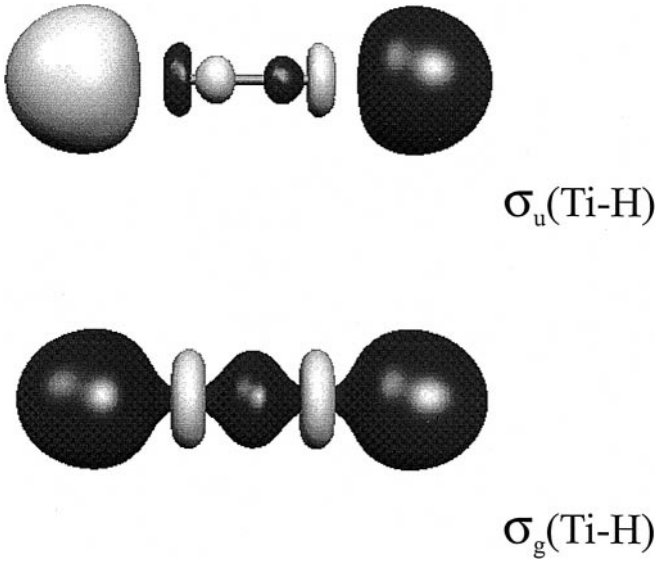

Fig. 6. Ti—H bonding orbitals of HTiTiH

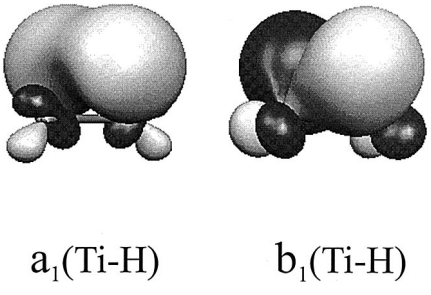

Fig. 7. Ti—H bonding orbitals of Ti(H,H)Ti

Table 7. Binding energies (kcal/mol) of the first and the second H atom in Ti_2H_2

	B3LYP	BLYP	BP86
First H			
$Ti_2 + H \rightarrow TiTiH$	56.4	54.3	56.2
$Ti_2 + H \rightarrow Ti(H)Ti$	60.2	61.6	65.8
Second H			
$TiTiH + H \rightarrow HTiTiH$	61.3	56.3	57.8
$Ti(H)Ti + H \rightarrow Ti(H,H)Ti$	67.0	66.8	69.1

titanium atoms in the located Ti_2H_6 and Ti_2H_8 structures [R(TiTi) is between 2.5 and 3.1 Å in these clusters].[2]

We saw in the previous section that the formation of the bridging Ti—H bonds in Ti_2H is slightly preferred over the terminal linkage. This is also the case for the binding of the second H atom. Table 7, where the binding energies of the first and the second hydrogen for the terminal and bridging structures are collected, shows that the energy of the $Ti(H)Ti + H \rightarrow Ti(H,H)Ti$ reaction is 6–11 kcal/mol larger than the energy of the $TiTiH + H \rightarrow HTiTiH$ reaction, providing an explanation for the enhanced stability of the Ti(H,H)Ti structure compared to HTiTiH.

3.5 Vibrational analysis for HTiTiH and Ti(H,H)Ti

The predicted harmonic vibrational frequencies and IR intensities of the HTiTiH and Ti(H,H)Ti forms of Ti_2H_2 are given in Table 8. Assuming that the BP86 functional gives reasonable frequencies for TiH stretching frequencies, the possibility of the existence of Ti_2H_2 among the matrix-isolated Ti_xH_y products is examined in this section.

From the two TiH stretching modes of HTiTiH, only the asymmetric combination (σ_u) is IR active. This band is predicted to be a rather intense absorption above 1500 cm^{-1}. If the HTiTiH molecule is isolated in rare-gas matrices then it is expected to give a sharp TiH stretching band since its geometry and its ground state are well defined (the molecule is not floppy and has no low-lying states). In the matrix study reported by Xiao et al. [7], a sharp band at 1512 cm^{-1} was observed when small titanium clusters were codeposited with molecular hydrogen. This band disappeared after the matrix was photolyzed with UV light. The calculated $\omega_2(\sigma_u) = 1548$ cm^{-1} is reasonably close to the observed frequency and the calculated $HTiTiH \rightarrow DTiTiD$ isotopic shift for this mode (H/D = 1.399) is also consistent with the experimental shift (H/D = 1.387). In the laser-ablation matrix study [8], several IR bands were observed around 1500 cm^{-1} and they were associated with Ti_xH_y species. Of these bands, the sharp absorption at 1485 cm^{-1} and its corresponding Ti/D_2 band at 1071 cm^{-1} did not shift when the reaction was made with mixed hydrogen (HD). On the basis of this observation, the authors suggested that the 1485 cm^{-1} band belongs either to a species involving a single H atom or to a molecule with two uncoupled hydrogens. The present calculations indicate that the motion of the two hydrogens in HTiTiH is coupled. The two TiH stretching modes are split by 31 cm^{-1} (Table 8); in line with this, the TiH stretching and TiD stretching frequencies of HTiTiD undergo notable shifts with respect to those

[2] B3LYP calculations with the present basis set predict that on the singlet potential-energy surface the quadruple-bridging Ti_2H_4 structure is 14 kcal/mol below the double-bridging form, and in both structures the TiTi bond length is around 2.1 Å. The titana analogue of the ethylene molecule (H_2TiTiH_2) is predicted to be a transition state far above the quadruple-bridging structure

Table 8. IR spectra of HTiTiH, Ti(H,H)Ti and their deuterated forms calculated using the BP86 functional: harmonic frequencies (cm^{-1}), IR intensities in *parentheses* (km/mol). The symmetry and the approximate description are given for each normal mode of the Ti_2H_2 forms. For the Ti(H,H)Ti molecule, the displacement of the H atoms in the b_1 TiH stretching mode is along the HXH plane, whereas the H atoms move parallel to the TiXTi plane in the b_2 TiH stretching mode (X denotes the midpoint of Ti_2)

		Ti_2H_2	Ti_2HD	Ti_2D_2
HTiTiH ($^1A_{1g}$)				
$\omega_1(\sigma_g)$	Symmetric TiH stretch	1579 (0)	1513 (335)	1128 (0)
$\omega_2(\sigma_u)$	Asymmetric TiH stretch	1548 (796)	1117 (220)	1106 (407)
$\omega_3(\pi_g)$	Asymmetric TiTiH bend	556 (0)	493 (23)	420 (0)
$\omega_4(\sigma_g)$	TiTi stretch	533 (0)	530 (0)	528 (0)
$\omega_5(\pi_u)$	Symmetric TiTiH bend	336 (211)	271 (130)	240 (108)
Ti(H,H)Ti ($^1A_1$)				
$\omega_1(a_1)$	TiH stretch	1383 (152)	1370 (126)	988 (73)
$\omega_2(b_1)$	TiH stretch	1356 (101)	976 (62)	964 (51)
$\omega_3(b_2)$	TiH stretch	1004 (12)	967 (7)	725 (7)
$\omega_4(a_2)$	TiH stretch	921 (0)	669 (2)	659 (0)
$\omega_5(a_1)$	HXH bend	668 (1)	581 (2)	475 (1)
$\omega_6(a_1)$	TiTi stretch	463 (9)	462 (9)	461 (9)
Ti(H,H)Ti ($^3B_1$)				
$\omega_1(a_1)$	TiH stretch	1374 (61)	1371 (85)	979 (30)
$\omega_2(b_1)$	TiH stretch	1369 (111)	977 (43)	976 (56)
$\omega_3(b_2)$	TiH stretch	1016 (11)	996 (6)	730 (6)
$\omega_4(a_2)$	TiH stretch	973 (0)	714 (2)	701 (0)
$\omega_5(a_1)$	TiTi stretch	433 (6)	432 (6)	431 (5)
$\omega_6(a_1)$	HXH bend	344 (18)	298 (14)	245 (9)

in HTiTiH and DTiTiD. For this reason, the assignment of the 1485 cm^{-1} band to HTiTiH can probably be ruled out, but this band may belong to TiTiH($^2\Delta$), for which we get $\omega_1(\sigma) = 1536\,cm^{-1}$ at the BP86 level (Table 6) with the corresponding TiTiD($^2\Delta$) prediction of $\omega_1(\sigma) =$ 1097 cm^{-1}.

The a_1 and b_1 TiH stretching frequencies of the bridging Ti_2H_2 molecule are predicted to be less intense than $\omega_2(\sigma_u)$ of HTiTiH, but they should still be quite strong absorptions in the 1350–1400 cm^{-1} region. The a_1 and b_1 combinations split up by only a few wavenumbers in the ground state of Ti(H,H)Ti and by almost 30 cm^{-1} in the $^1A_1$ state. With high Ti concentration, Xiao et al. observed a broad feature in this part of the IR spectra with a sharp band at 1396 cm^{-1}, which disappeared after UV photolysis. This latter band or/and other bands in the broad feature could be due to Ti(H,H)Ti. The 1350-1400 cm^{-1} region is rather simple in the spectra of Chertihin and Andrews [8]. Only a doublet at 1385/ 1389 cm^{-1} was observed; the intensity of the 1385 cm^{-1} peak depended strongly on the laser power. The 1389 cm^{-1} band was assigned to HO_2 and from a comparison with Hartree–Fock calculations the 1385 cm^{-1} band was associated with the TiH dimer. As noted before, both high-quality ab initio and DFT calculations give much higher frequencies for the ground state of TiH. If this band is not due to TiH then it may belong to another Ti_xH species with $x > 1$ because its isotopic behavior is consistent with a product with a single H atom. Any of the $^4B_1$ and $^2B_1$ states of Ti(H)Ti would be a good candidate for this species since their predicted a_1 TiH stretching frequencies match well with the observed frequency. In this case, however, one should observe another band either around 1000 cm^{-1} ($^4B_1$ state) or around 1100 cm^{-1} ($^2B_1$ state) with a comparable intensity as the 1385 cm^{-1} peak (Table 6). Some bands are indeed listed in Table I of Ref. [8], but they were associated with HO_2 and TiO species.

4 Summary and concluding remarks

Although the HTiTiH isomer of Ti_2H_2 with two terminal hydrogens and the triple metal–metal bond is found to be thermodynamically stable with respect to $Ti_2 + H_2$, this structure does not represent the global minimum on the Ti_2H_2 potential-energy surfaces. In spite of the similarity of the valence electron shells of Ti and C atoms, the first two hydrogens prefer to bind to Ti_2 in the bridging position. That is why the bridging Ti(H,H)Ti isomer is notably more stable than the HTiTiH form. For more saturated Ti_2H_{2n} species ($n = 2$ and 3), the titana-hydrocarbon structures (H_2Ti-TiH_2 and H_3TiTiH_3) do not seem to be stable [9].

A comparison of the predicted IR spectra with those recorded in the Ti_x/H_2 matrix isolation studies provides an indication that both HTiTiH and Ti(H,H)Ti species might have been formed in low-temperature experiments; however, it is quite clear from the discussion presented in Sect 3.5 that at present it is impossible to give definite assignments for the observed bands. All the statements there should be considered as only probability statements. Further careful experimental and theoretical work is required to be able to identify, if they can be at all, the Ti_2H and Ti_2H_2 species.

Finally, it should be pointed out that the present work was not meant to provide accurate energetic and structural properties for Ti_2H_2. Although no sign of multireference problems (symmetry breaking, unusual harmonic frequencies, spin contamination) was encountered for the molecules investigated, it is quite likely that nondynamic electron correlation contributions

should be taken into account to obtain reliable predictions. The present results, however, may serve as a starting point for more demanding calculations.

Acknowledgements. Financial support from the Hungarian Academy of Sciences (AKP, 97-102 2,4/32) and from the Hungarian Research Foundation (OTKA, T029926) is gratefully acknowledged.

References

1. Lee YK, Manceron L, Pápai I (1998) J Phys Chem 101: 9650
2. Breisacher P, Siegel B (1963) J Am Chem Soc 85: 1705
3. Jolly CA, Marynick DS (1989) Inorg Chem 28: 2893
4. Thomass JR, Quelch GE, Seidl ET, Schaefer HF III (1992) J Chem Phys 96: 6857
5. Kudo T, Gordon MS (1995) J Chem Phys 102: 6806
6. Ma B, Collins CL, Schaefer HF III (1996) J Am Chem Soc 118: 87
7. Xiao ZL, Hauge RH, Margrave JL (1991) J Phys Chem 95: 2696
8. Chertihin GV, Andrews L (1994) J Am Chem Soc 116: 8322
9. Webb SP, Gordon MS (1995) J Am Chem Soc 117: 7195
10. Garcia A, Ugalde JM (1996) J Phys Chem 100: 1227
11. Webb SP, Gordon MS (1998) J Am Chem Soc 120: 3846
12. Frisch MJ, Trucks GW, Schlegel HB, Gill PMW, Johnson BG, Robb MA, Cheeseman JR, Keith T, Petersson GA, Montgomery JA, Raghavachari K, Al-Laham MA, Zakrzewski VG, Ortiz JV, Foresman JB, Peng CY, Ayala PY, Chen W, Wong MW, Andres JL, Replogle ES, Gomperts R, Martin RL, Fox DJ, Binkley JS, Defrees DJ, Baker J, Stewart JP, Head-Gordon M, Gonzalez C, Pople JA (1995) Gaussian 94. Gaussian, Pittsburgh, Pa
13. Schäfer A, Horn H, Ahlrichs R (1992) J Chem Phys 97: 2571
14. Wachters AJH (1970) J Chem Phys 52: 1033
15. Hay PJ (1977) J Chem Phys 66: 43
16. Becke AD (1993) J Chem Phys 98: 5648
17. Lee C, Yang W, Parr RG (1998) Phys Rev B 37: 785
18. Becke AD (1988) Phys Rev A 38: 3098
19. (a) Perdew JP (1986) Phys Rev B 33: 8822; (b) erratum in (1986) Phys Rev B 34: 7406
20. Schlegel HB (1982) J Comput Chem 3: 214
21. Huber KP, Herzberg G (1986) Molecular spectra and molecular structure IV. Constants of diatomic molecules. Van Nostrand Reinhold, Toronto
22. Salahub DR (1987) Adv Chem Phys 69: 447
23. Bauschlicher CW (1991) J Chem Phys 95: 1057
24. Bergström R, Lunell S, Eriksson LA (1996) Int J Quantum Chem 59: 427
25. Doverstål M, Lindgren B, Sassenberg U, Arrington CA, Morse MD (1992) J Chem Phys 97: 7087
26. Cossé C, Fouassier M, Mejean T, Tranquille M, DiLella DP, Moskovits M (1980) J Chem Phys 73: 6076
27. Barone V, Adamo C (1997) Int J Quantum Chem 61: 443
28. Launila O, Lidgren B (1996) J Chem Phys 104: 6418
29. Chong DP, Langhoff SR, Bauschlicher CW, Walch SP, Partridge H (1986) J Chem Phys 85: 2850
30. Bauschlicher CW (1988) J Phys Chem 92: 3020
31. Anglada J, Bruna PJ, Peyerimhoff SD (1990) Mol Phys 69: 281
32. Bogey M, Bolvin H, Cordonnier M, Demuynck C, Destombes JL, Császár AG (1994) J Chem Phys 100: 8614
33. Flükiger P (1992) PhD thesis, University of Geneva
34. Mayer I (1983) Chem Phys Lett 97: 27
35. Mayer I (1986) Int J Quantum Chem 29: 73
36. Mayer I (1986) Int J Quantum Chem 29: 477